10.21611/qirt.2023.26

Quantitative Analysis of Pedal Ulcerations Using Thermographic Images

Dhanalakshmi M, Deepa Rohini T, Fowziya Begum A and Komatheswari T

Sri Sivasubramaniya Nadar College of Engineering, kalavakkam-603110, Tamilnadu, India.
dhanalakshmim@ssn.edu.in

ABSTRACT

Thermographic images are widely used in diagnosing Diabetic foot (DF) infection and ulceration that are associated with neurological abnormalities. Thermographic images of various diabetic foot ulcerated conditions are collected from 60 patients. There are twenty different types of conceptual foot patterns occurring in diabetic patients, out of which most predominantly observed are type 3A, type 1D, type 3D, type 4D. This work proposes on developing an automatic algorithm to match these diabetic thermographic images of ulcerated foot with conceptual template rather than manually comparing it with the thermogram datasheet. A conceptual template is created using the thermogram datasheet for each of these twenty patterns by edge mapping and curvelet technique. About 60 thermographic images of diabetic foot that have the most predominant patterns are taken for study. These images are pre-processed and segmented for ulcerated region of interest. A pattern for these thermographic images is generated using edge mapping technique and Hough transform. The broken edges are joined by curvelet technique to form a pattern. Each of these patterns is compared with the twenty conceptual templates by template matching technique and an overall efficiency of about 95.27 percent is achieved. This automated algorithm helps the physicians in finding the accurate type of diabetic foot and it is possible to detect the pre-signs of ulcerations in foot.

1. Introduction

High blood sugar levels, or hyperglycaemia, are a defining feature of diabetes. [1]. The quantity of sugar that insulin transports from the blood into the body determines how much of it there is [2]. Depending on the degree of hyperglycaemia, diabetes is categorized into many categories:

- Type 1 diabetes, is an autoimmune disease which generally affects young age people and children. It causes the loss of insulin producing cells.
- Type 2 diabetes mainly affects adults. It occurs because the cells do not respond properly to insulin.
- Type 3 affects age above 30. The ability to produce insulin is affected due to damage in pancreas
- Type 4 diabetes occurs due to ageing.

Diabetic foot ulcers occur (DFUs) occur in diabetic patients commonly as they have low blood circulation to their feet. Diagnosis of DFUs is usually inflammation, wound, formation of black tissue, itching etc.,[3]. People with diabetes time and again encounter with these difficulties, combat infections due to DFU. These foot problems are the main reason for lower limb amputation all over the world. DFUs is eventual for up to 85% for loss of lower extremity [4, 5, 6]. Thermography is a potential technique for identifying ulcers. An infrared camera is used in the diagnosis of diabetes type by observing the changes in temperature in foot. In spite of technology availability in identifying disease using tissue examination and magnetic resonance imaging, still it is difficult to for the subjects to undergo these test procedures as it is either invasive or create MRI phobia. Our proposal is to develop a unique method in order to classify the severity of the condition by comparing the processed thermogram with the theoretical patterns of diabetic feet.

There has been extensive research in thermographic images to detect diabetic foot. The thermal images acquired using infrared camera are investigated to determine thermal spread in spatial domain. An automated method using thresholding, histogram, clustering, object-attribute identification and entropy methods were used for segmentation [7]. Makotooe et. al., performed investigations with diabetic and osteomyelitis patients and analyzed the skin temperature. They found an ankle pattern for analysis which provided an optimistic predictive value for examining osteomyelitis patients [8]. There were other approaches using automatic segmentation of Region of Interest (ROI) followed by extraction of features. Canny edge detection, Gabor filter and region growing are popularly used in determining the ROIs. Texture color features and HOG (Histogram of Oriented Gradients) features are used widely to classify type of diabetic foot [9, 10]. Patel et al. [10] developed an architecture to identify diabetic foot ulcers. The architecture consists of pre-processing, segmentation, extracting feature sets and classification. They processed the images using HIS color spaces first, after which they found textures and categorized them.

More recently automated classification accelerates the treatment process and enhance the patient's health. Kaplan et al. [11] used MRI images achieved a high accuracy using K-Nearest Neighbour (KNN) model with 95.56%. Liu et al. [12] published EfficientNet and all available baselines. Additionally, an efficient DFU dataset is produced using color images in order to perform a two-class classification. This method offers classification accuracy for ischemia and infection of 99% and 98%, respectively. Apart from conventional approaches, machine learning has emerged as a prominent technology for the analysis of vast datasets. In the realm of classification tasks, several noteworthy techniques have gained

prominence, including EfficientNet, Visual Geometry Group (VGG) Nets, GoogleNet, and AlexNet. In one instance, Das et al. [13] harnessed a shared decoder and a pyramid-like loss (SPNet) network, which incorporated both global and local features. Remarkably, this approach yielded an impressive accuracy rate of 97.4%. Similarly, Stefanopoulos et al. [14] devised a unique method for anticipating neuropathic ulcers in diabetic patients. This method relied on a "CTREE" decision tree and involved an evaluation of six pertinent factors to determine the likelihood of developing neuropathic ulcers. Impressively, the CTREE model exhibited remarkable performance metrics, with a recall rate of 0.806, precision of 0.783, accuracy of 0.789, and an Area Under the Curve of 0.88.

In spite of the emergence of new technologies, the assessment of foot thermograms still relies on clinical evaluation to ascertain the specific type of diabetes. However, locating qualified clinicians for this task can be challenging. Consequently, several research investigations have been dedicated to creating an automated DFU recognition system. Regrettably, only a limited number of these studies have incorporated foot thermograms [15, 16]. The primary objective of this proposed study is to develop a unique method capable of performing template matching on thermographic images of diabetic patients, thereby determining the diabetes type without the need for verifying extensive data sheets. To achieve this, the study employs segmentation and employs the curvelet technique to identify distinct patterns associated with diabetes. These patterns are then applied to edge-mapped conceptual templates, enabling the precise identification of the diabetic type.

2. Materials and Methods

The database used for the present work and the development procedures for the automated diabetic type diagnosis algorithm utilizing plantar thermal images are presented below. Figure 1 demonstrates the blocks involved in the present work.

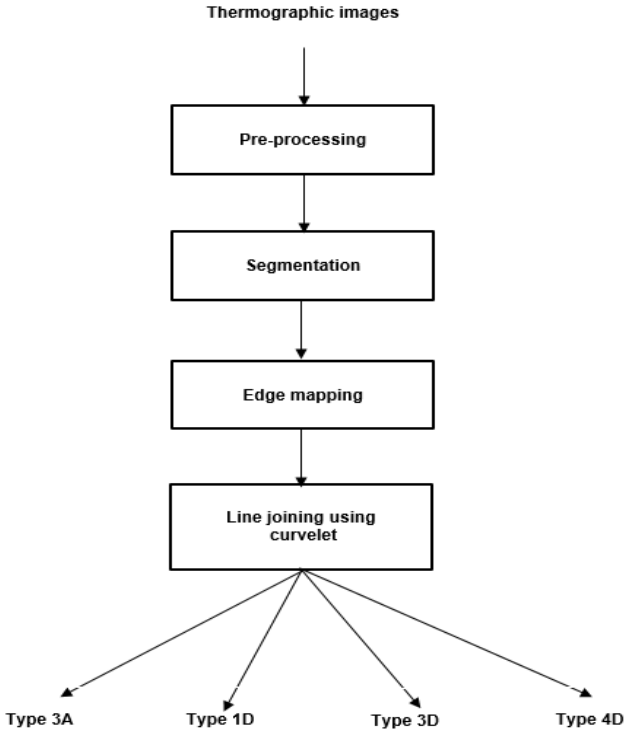

Fig.1. *Flow chart of the proposed methodology*

2.1 Data Collection

A variety of thermographic foot patterns were recorded from 60 individuals at the CGN research labs in Tirupati and saved as bitmap files. Following the examination of 80 images, 19 were categorized as Type I, 35 as Type III, and 26 as Type IV. The physiological imaging IR-Analysis software (Version.1.0) is then used to examine them. The next step is to extract JPG images using a bitmap to JPG converter.

2.2 Diabetic foot patterns

Most commonly occurring foot patterns among diabetic patients are shown below in figures 2 to 5 [17]. The complete flow and occlusions in the Lateral Plantar Artery (LPA), Lateral Calcaneal Artery (LCA), Medial Plantar Artery (MPA), and Medial Calcaneal Artery (MCA) for different types of diabetic foot are represented here. In most of the types MCA and LCA are blocked in the heel area.

(i) Type:3A

Fig. 2. *Type3A - The LPA and LCA are intact, but the MPA and MCA are all blocked. Foot: Only the LPA angiosome is intact, and the MPA is blocked.*

(ii). Type:1D

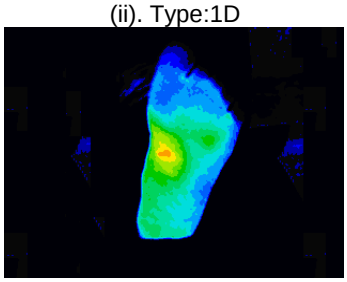

Fig. 3. *Type 1D - MPA, MCA, LCA and LPA are occluded. Forefoot: MPA and LPA are intact-Normal "butterfly pattern".*

(iii) Type: 3D

Fig. 4. *Type 3D - LPA is intact, however MPA, MCA, and LCA are all blocked. Foot: Only the LPA angiosome is intact, and the MPA is blocked.*

(iv) Type:4D

Fig. 5. *Type 4D – MCA, LCA, and LPA are blocked, and MPA is intact. Foot: Only the MPA angiosome is intact, and the LPA is blocked.*

2.3 Pre-processing

In this work, filtering techniques are studied in order to remove thermal noise from the collected thermographic images and to choose the best filter among three filters (Weiner filter, shock filter, and Gaussian filter) based on the parameters mean square error (MSE), root mean square error (RMSE), peak signal to noise ratio (PSNR), and mean absolute error (MAE). All input images of type 3A, type 1D, type 3D, and type 4D are pre-processed to reduce noise. The purpose of the noise reduction class of filters is to remove outlier or extreme values from areas of an image where the values should be generally uniform.

(a) (b) (c)

Fig. 6. *Filtered image using (a) Wiener filter (b) Shock filter and (c) Gaussian filter*

The best filter is estimated based on the four parameters listed in table 1. From the table it is clear that Gaussian filter with high PSNR, low MSE, low MAE and low RMSE gives best Result.

Table 1. *Validation of filters*

FILTER	PSNR	RMSE	MAE	MSE
WIENER	+21.6963db	1.409	139.521	0.00675
GAUSSIAN	+30.8192db	0.55785	32.794	0.00082
SHOCK	-20.5729db	10.6819	159.645	114.10366

2.4 Segmentation

In this work the affected ulcerated region is segmented from the pre-processed image. The technique of segmenting an image into separate parts based on their numerous properties and extracting the most interesting target is known as image segmentation. In our study the following algorithms are extensively used to derive the Region of Interest (RoI): K- means algorithm, Active contour segmentation, LSM & fuzzy clustering, and Watershed segmentation.

2.4.1 Image segmentation using K-means algorithm

Basic image segmentation tasks is performed using the well-known K-Means clustering technique. It divides the space and also divides the outer region of the foot. The objective of this convergent clustering algorithm is to maximize the partitioning decisions made in response to an initial set of clusters that is supplied by the user. The following steps are involved in the process:

- Selecting the number of clusters as k
- Partitioning data set by assigning data point to clusters based on Euclidean distance
- Recalculate cluster center
- Repeat the above two steps until the data points are not assigned to different clusters

Using these steps, the thermographic image is segmented based on RGB color space. figure 7 displays the segmented image of type 3A produced by the K-Means clustering technique.

Fig.7. *Sample Type 3A thermographic image after color segmentation.*

2.4.2 Active contour segmentation

The segmentation process involving active contour methods is efficient because it employs dynamic curves to segment the boundaries of objects within an image. In this case, the Chan-Vese active contour segmentation approach is utilized to segment the image. This method achieves segmentation by identifying a contour that divides the given image into distinct, non-overlapping regions. The algorithm minimizes an energy function that comprises weighted values. These values represent the cumulative sum of variations in intensity compared to the average value outside the delineated area, the cumulative sum of differences from the average value within the delineated area, and a component linked to the length of the boundary surrounding the delineated region. This minimization process is carried out iteratively and is based on evolving level sets. Figure 8 illustrates the segmented image of type 3A achieved through Chan-Vese active contour segmentation.

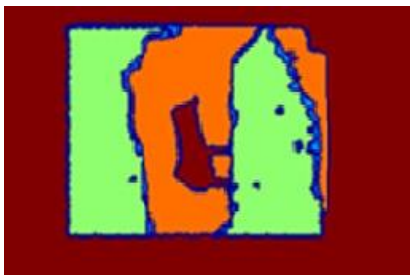

Fig.8. *Sample Type 3A thermographic image after color segmentation*

2.4.3 LSM and Fuzzy Clustering

The level set method (LSM) is a commonly employed approach for image segmentation. It enables the representation of hypersurfaces, like curves or surfaces, in various dimensions by establishing a zero-level set of characteristic points. Within the realm of image segmentation, the fuzzy level set method (FLSM) serves as an extension of LSM. FLSM integrates the automatic initiation of the initial contour and parameter setup from fuzzy c-means (FCM), all while maintaining its core functionality as a level set method.

Fig. 9. Sample Type 3A segmented using LSM and fuzzy clustering

A significant enhancement in FLSM involves the incorporation of a "fuzziness index" into the objective function. This index is in line with the notion of fuzzy partitioning employed in FCM. In this context, each area of interest within the image, corresponding to each cluster center, encompasses a group of image pixels with membership-degree values that fit within the interval defined by the cluster center. By ascertaining the initial categories and constructing approximate initial contours for all regions of interest, FLSM strives to avert inadequate evolution or excessive segmentation. Figure 9 provides a visual representation of the segmented image of type 3A achieved through LSM and fuzzy clustering.

2.4.4 Watershed Segmentation

The watershed transform operates by simulating how topographic surface is conceptualized. In this analogy, the image is imagined as a topographic surface that gradually floods from the lowest to the highest points, much like water filling a basin. As the flooding process recurs, it creates natural boundaries called watersheds. In the context of image segmentation, the gradient of the image is applied to a watershed transform. The watershed lines then serve as dividers between regions with similar characteristics or properties. Figure 10 provides a visual representation of image segmentation using the watershed technique.

Fig.10. *Segmented image using watershed method*

In this study, K-means clustering algorithm provides the best segmentation result without any loss in the region of interest. For the 80 pre-processed images, the diabetic foot images of types 3A, 1D, 3D, and 4D are segmented using this K-means method.

2.5 Edge Extraction

The process of extracting prominent edge segments from color images of diabetic feet is depicted in figure 11. The initial step in edge detection focuses on determining the significance of edge pixels in terms of perception. Edge pixels randomly scattered across our generated edge map do not offer meaningful insights into the original image's edges until they are organized and processed.

To address this, Hough transform is employed on the edge map, which aids in connecting edge pixels that belong to the similar connecting lines. While the Hough transform is effective at detecting pixels aligned along straight lines, it's possible for multiple line segments to share pixels along the similar line. Hence, the primary goal of the line segment extraction stage is to identify and distinguish these individual line segments. Additionally, short line segments are removed, as they might be considered noise or of minimal interest to the user.

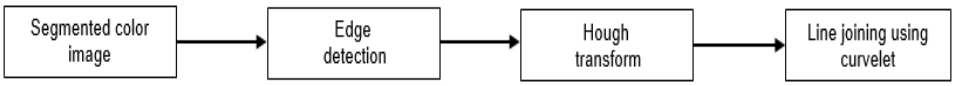

Fig. 11. *Processing stage for prominent edge extraction*

2.5.1 Canny edge detection

When conducting edge detection, partial derivatives are used to compute changes in color (or intensity in the case of grayscale images) in pixel level. Nevertheless, it's worth noting that derivatives have a tendency to amplify visual disturbances. To address this issue, Canny edge detection technique is adopted to identify edges within the segmented image. This technique identifies edges by identifying local peaks in the gradient of the function f(x, y). The gradient itself is derived from a Gaussian filter. The approach selectively highlights faint edges only when they are associated with robust edges, utilizing two criteria to distinguish between strong and weak edges.

2.5.2 Hough Transform

The primary goal of using Hough transform is to identify improper occurrences of objects associated with specific shapes through a voting mechanism. This voting process occurs within a parameter space, and potential object points are recognized as peak points within an accumulator space explicitly generated by the Hough transform algorithm.

In the context of automated analysis of digital images, there is often a necessity to detect fundamental shapes like straight lines, circles, or ellipses. To accomplish this task, an edge detector is frequently employed as an initial step to find pixels situated along the anticipated lines in the homogeneous regions. However, due to possible inadequacies in the edge detection algorithm or the data, there may be cases where the intended lines have missing pixels. The challenge of aligining the determined edge features into suitable geometric shapes is effectively performed by the Hough transform. It achieves this by facilitating the grouping of pixels in the curves into potential object points through a specific voting procedure applied to a collection of parameterized image objects.

2.5.2 Line joining using Curvelet Transform

While the Hough transform is effective at determining which pixels lie along straight lines, it may identify pixels that are not necessarily connected, potentially belonging to multiple line segments along the same straight line. To address this issue, the line segment extraction process aims to achieve two primary objectives. First, it focuses on examining the pixel continuity, seeking to identify subsets of pixels that exclusively pertain to a single line segment. This involves assessing how closely successive pixels are aligned along a straight line. Secondly, the process aims to enhance the quality of the edge map by eliminating small line segments that contribute to noise or are deemed unnecessary. To achieve this, it measures the distance between two consecutive points concerning the line formed by the pixels along a straight line. To enhance the precision of our line segment extraction, a strategy known as the "greedy approach" is implemented. This strategy entails removing line segments that are adjacent to longer segments with closely matching orientations. Before executing this procedure, the line segments are arranged in descending order of length.

The likelihood that this cluster of line segments originates from the same curvelet (and thus should be combined as a group), can be expressed as a function of the noise model and curvelet feature set. This probability serves as a measure of how effectively a specific curvelet structure represents a collection of data points. Importantly, it is not influenced by the relative arrangement of data points along the given line segments but is determined solely by the geometric structure inherent in the dataset.

2.5.3 Template Matching

This is a process used to search for images that resemble a given template image. It involves selecting suitable points by sampling. One can lessen the sampled points by decreasing the resolution of both source and template images by the one common factor and then applying the matching task to the resulting scaled-down images. Two primary components are required for template matching:

1. Original image (I): The image in which a match to the template image is anticipated
2. Template (P) : The image that will be compared to the original image.

In the realm of simple template matching techniques, a convolution mask is employed to match certain characteristics within a search image that is aimed to be detected. This method is particularly well-suited for grayscale or edge images. This technique typically starts by choosing a portion of the search image as an initial patten. The search image and the template image are denoted as $I(x, y)$ and $P(x_t, y_t)$ respectively. The process involves computing the total of the coefficients' products in $I(x, y)$ and $P(x_t, y_t)$ across the entire area covered by the template. It is achieved by systematically shifting the center (or origin) of $P(x_t, y_t)$ across each point (x, y) in the search image. Since it considers all potential pixel value for the template in relation to the search image and eventually identifies the most suitable match, the highest scoring pixel value is considered the optimal location.

3. Results

The proposed work focuses to develop an automated algorithm to perform quantitative analysis of diabetic foot ulcerations by processing thermographic images. The ulcerated region are segmented and the edges are extracted to generate templates to match with the patterns of diabetic foot. The template matching patters are generated with algorithm specified in Section 2.5.3.

Figure 12 shows the templates of twenty different diabetic foot patterns used for template matching. These templates are generated using edge mapping technique. The most predominant patterns of thermographic diabetic foot are matched with these conceptual patterns.

The original images are pre-processed, segmented and edge detected based on the methods discussed in Sections 2.3 to 2.5. These images are mapped to the conceptual templates generated. The results are classified into type 3A, type 1D, type 3D and type 4D as shown in figures 13 to 16.

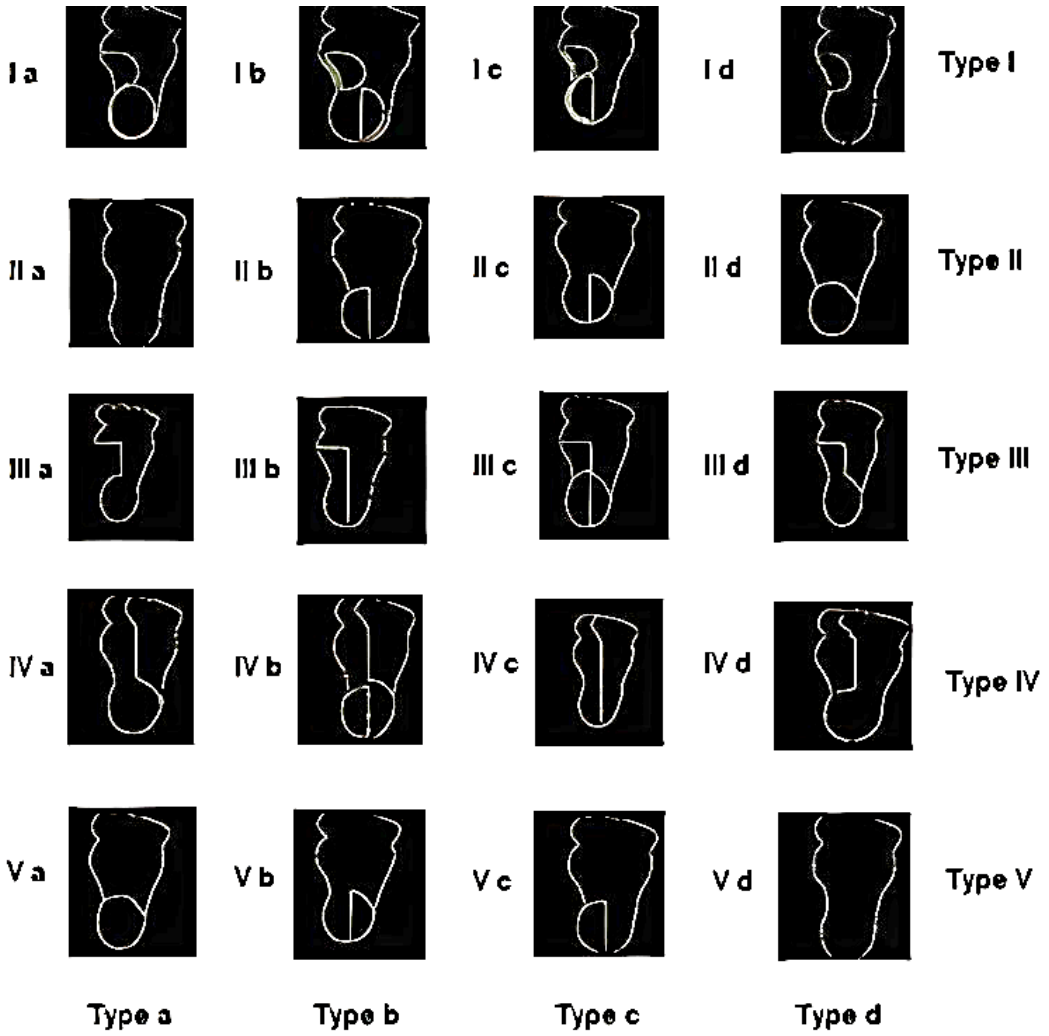

Fig.12. Templates for diabetic foot

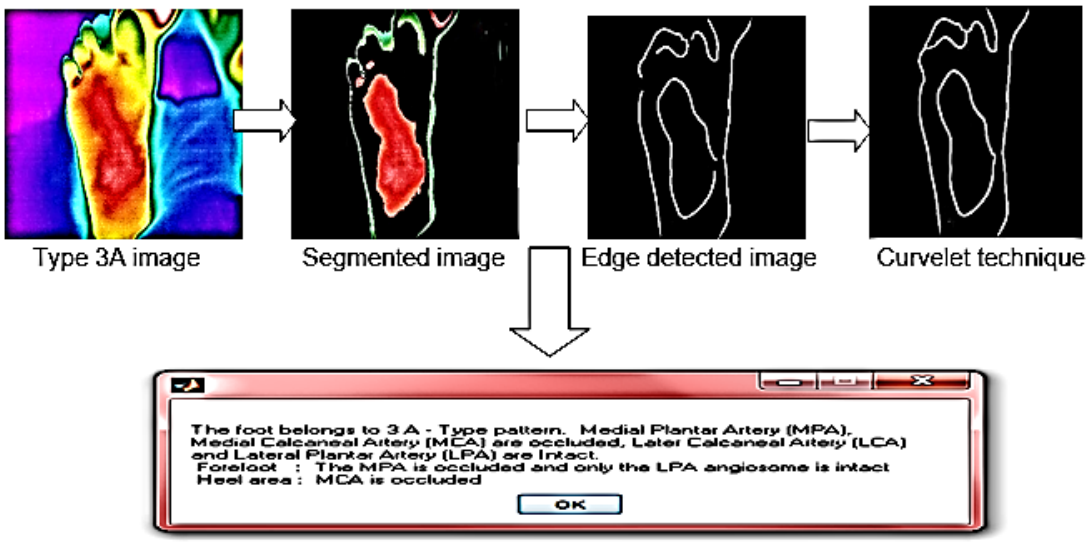

Fig. 13. *Template matched outcome for a type 3A image*

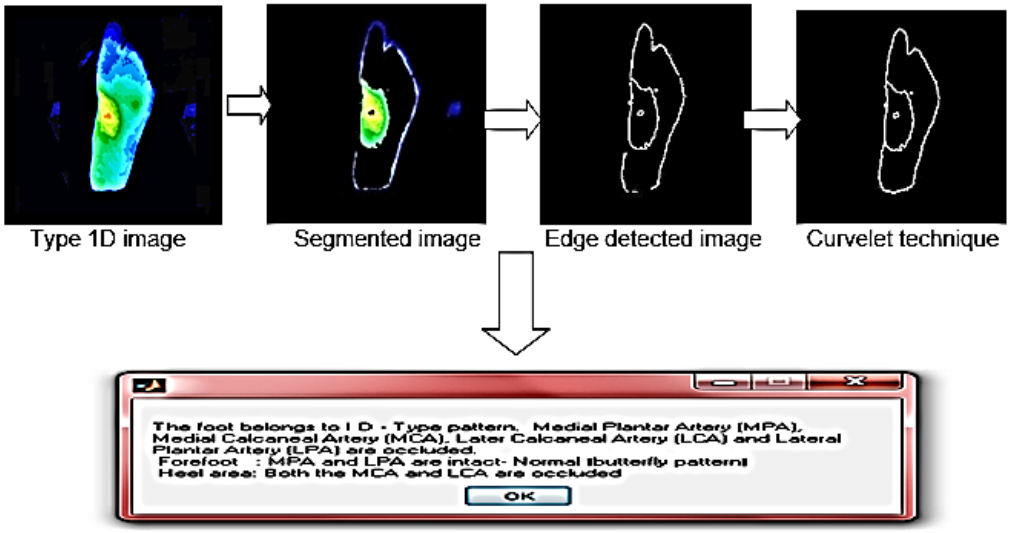

Fig. 14. *Template matched outcome for a type 1D image*

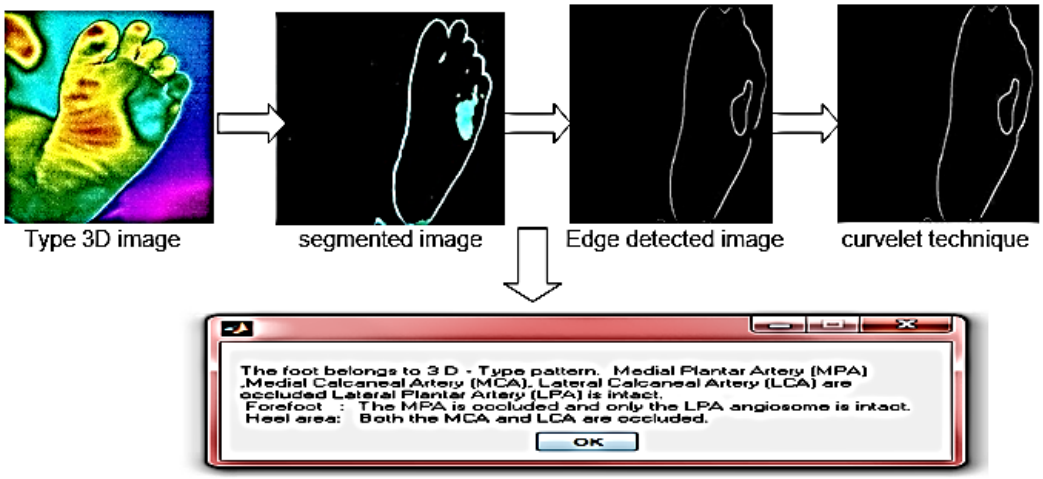

Fig. 15. Template matched outcome for a type 3A image

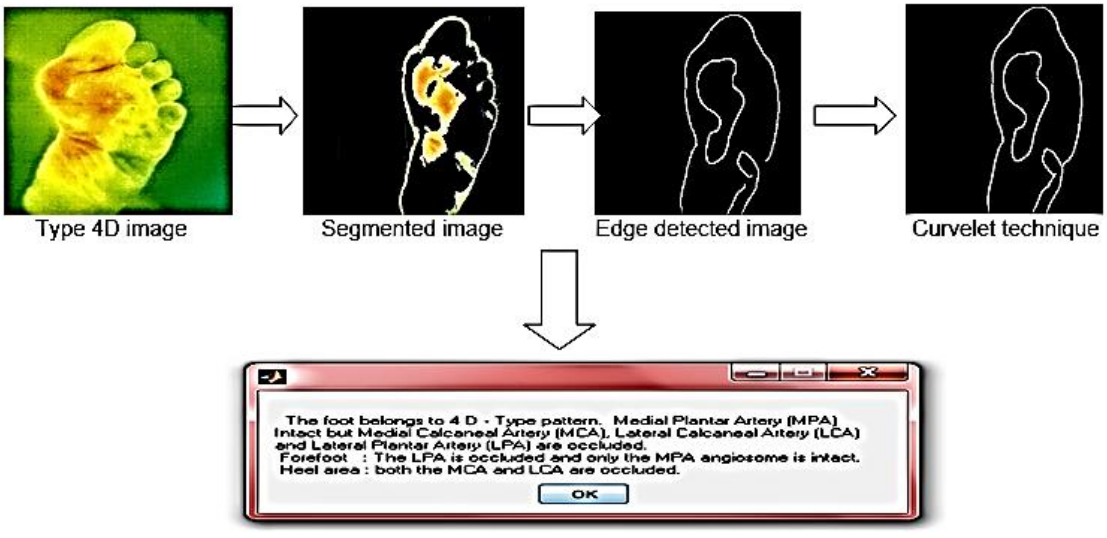

Fig. 16. Template matched outcome for a type 4D image

4. Conclusion:

An attempt was made to formulate a unique method to match the real time thermographic diabetic foot images with the conceptual templates and classify the four most commonly occurring patterns of diabetic foot ulceration. It eliminates the operator dependency and improves the diagnostic approach. The template matching thus helps the physicians in finding the accurate type of diabeticfoot and it is possible to detect the pre-signs of ulcerations. The given input image is matched with the conceptual templates and the overall efficiency of about 95.27percent is achieved.

5. REFERENCES

[1] Das, S.K., Roy, P., Mishra, A.K. Deep learning techniques dealing with diabetes mellitus: A comprehensive study. In Health Informatics: A Computational Perspective in Healthcare, Springer: Singapore, pp. 295–323, 2021

[2] Health Organization. WHO Expert Committee on Diabetes Mellitus: Second Report, WHO Technical Report Series 646, World Health Organization: Geneva, Switzerland, 1980.

[3] Shailaja, K., Seetharamulu, B., Jabbar, M.A. Machine learning in healthcare: A review. In Proceedings of the 2018 Second International Conference on Electronics, Communication and Aerospace Technology (ICECA), Coimbatore, India, 29–31 March 2018.

[4] Qayyum, A., Qadir, J., Bilal, M., Al-Fuqaha, A. Secure and robust machine learning for healthcare: A survey. IEEE Rev. Biomed. Eng. Vol.14, 156–180, 2020.

[5] Giger, M.L. Machine learning in medical imaging. J. Am. Coll. Radiol. Vol.15, pp.512–520, 2018.

[6] Mishra, A.K., Roy, P., Bandyopadhyay, S., Das, S.K. Breast ultrasound tumour classification: A Machine Learning—Radiomics based approach. Expert Syst. Vol.38, e12713, 2021.

[7] ChanjuanLiua, Ferdi van der Heijden, Marvin E. Klein, Jeff G. van “Infrared Dermal Thermography on Diabetic Feet Soles to Predict Ulcerations: a Case Study” Vol. 8572, 85720N • © 2013 SPIE CCC code: 1605-7422/13/$18 • doi: 10.1117/12.2001807, pp.1-9, 2013.

[8] Makotooe, Rie Roselyne Yotsu, Hiromi Sanada, Takashi Nagase, and Takeshi Tamaki, “Screening for Osteomyelitis Using Thermography in Patients with Diabetic Foot”, Hindawi Publishing Corporation Research Article ID 284294, pp. 1-6, 2013.

[9] Pragati Kapoor S. V. A. V. Prasad Seema Patni, “Image Segmentation and Asymmetry Analysis of Breast Thermograms for Tumor Detection”, International Journal of Computer Applications (0975 – 8887) Volume 50 – No.9,.pp. 40-44, 2012.

[10] Patel, S., Patel, R., Desai, D. Diabetic foot ulcer wound tissue detection and classification. In Proceedings of the 2017 International Conference on Innovations in Information, Embedded and Communication Systems (ICIIECS), Coimbatore, India, pp. 1–5, 17–18 March 2017,

[11] Kaplan. K, Kaya. Y, Kuncan. M, Ertunç, H. M, Brain tumor classification using modified local binary patterns (LBP) feature extraction methods Med. Hypotheses, Vol.139, Article 109696, 2020.

[12] Liu, Z., John, J., Agu, E. Diabetic Foot Ulcer Ischemia and Infection Classification Using EfficientNet Deep Learning Models. IEEE Open J. Eng. Med. Biol. Vol.3, 189–201, 2022.

[13] Das, S.K., Roy, P., Mishra, A.K. DFU_SPNet: A stacked parallel convolution layers based CNN to improve Diabetic Foot Ulcer classification. ICT Express Vol.8, 271–275, 2021.

[14] Stefanopoulos, S., Ayoub, S., Qiu, Q., Ren, G., Osman, M., Nazzal, M., Ahmed, A. Machine learning prediction of diabetic foot ulcers in the inpatient population. Vascular, 30, 17085381211040984, 2021.

[15] Cruz-Vega, I., Hernandez-Contreras, D., Peregrina-Barreto, H., Rangel-Magdaleno, J.d.J., Ramirez-Cortes, J.M. Deep Learning Classification for Diabetic Foot Thermograms. Sensors, Vol.20, 1762, 2020.

[16] Adam, M., Ng, E.Y.K., Oh, S.L., Heng, M.L., Hagiwara, Y., Tan, J.H., Tong, J.W.K., Acharya, U.R. Automated8Detection of Diabetic Foot with and without Neuropathy Using Double Density-Dual Tree-Complex Wavelet Transform on Foot Thermograms. Infrared Phys. Technol. Vol.92, 270–279, 2018.

[17] Nagase T, Sanada H, Oe M, Takehara K, Nishide K, Kadowaki T. Screening of foot inflammation in diabetic patients by non-invasive imaging modalities. InGlobal Perspective on Diabetic Foot Ulcerations, Dec 9. IntechOpen, 2011.